Supporting Information

Facile preparation of phospholipid- amorphous calcium carbonate hybrid nanoparticles: toward controllable burst drug release and enhanced tumor penetration

Cheng Wang [a], Xuerong Liu [a], Shaoqing Chen [a], Fuqiang Hu [a],
Jihong Sun [b,*], Hong Yuan [a,*]

[a] *College of Pharmaceutical Sciences, Zhejiang University, 866 Yuhangtang Road, Hangzhou, 310058, China*
[b] *Sir Run Run Shaw Hospital, School of Medicine, Zhejiang University, No. 3 Qingchun East Road, Hangzhou, 310016, China*

* Corresponding authors.
E-mail: braversun@sina.com (Jihong Sun) and yuanhong70@zju.edu.cn (Hong Yuan)

03 Sep 2020

Note added after first publication: This Supplementary Information file replaces that originally published on 25 Oct 2018. The authors regret that Fig. S2 (image of ACC), Fig. S9C and Figure S13 (spleen image of PL/ACC-DOX and PL/CCC-DOX and lung image of PL/CCC-DOX) in the original file were incorrect due to errors in image processing. This new version includes the correct images. This does not affect the results or conclusions of the article.

Experimental Section

***Materials*:** Ammonium carbonate ($(NH_4)_2CO_3$) and anhydrous calcium chloride ($CaCl_2$) were purchased Sinopharm Chemical reagent Co., LTD (Shanghai, China). Doxorubicin hydrochloride (DOX) was a gift from Dalian Meilun Biotech Co., Ltd. (Dalian, China). Oleic acid (OA), phospholipid (PL, S100) and 1,2-Distearoyl-snglycero-3-phosphoethanolamine-N-[methoxy(polyethylene glycol)-2000] (DSPE-PEG_{2000}) were obtained from Lipoid GmbH (Ludwigshafen, German). DSPE-PEG-FA (35000 Da) was obtained from Ponsure Biotechnology (Shanghai, China). Hoechst 33342, propidium iodide (PI), methyl thiazolyl tetrazolium (MTT), coumarin 6 (C6), DiR, Lyso tracker Blue and Fluo-4 AM were obtained from Thermo Fisher Scientific (MA, USA). All other chemicals and reagents otherwise stated were from Sinopharm Chemical reagent Co., LTD and of analytical grade.

Cell culture: HeLa (human cervical carcinoma) was a gift from Dr. Pengfei Cui (China Pharmaceutical University). A549 (human lung carcinoma) and NIH3T3 (mouse embryonic fibroblast) cell lines were purchased from Institute of Biochemistry and Cell Biology (Shanghai, China). All cells were cultured in folate free dulbecco's modified eagle medium (DMEM, Sigma, USA) supplemented with 10% (v/v) fetal bovine serum (FBS, Hyclone, USA), 100 U/mL penicillin and 100 μg/mL streptomycin (Beyotime Biotechnology, China) in a humidified atmosphere of 95% air/5% CO_2 incubator (Thermo Forma 311, Thermo Scientific, USA) at 37 °C. All experiments were performed on cells in the logarithmic phase of growth.

Multi-cellular tumor spheroid model (MCTS): A 96-well plate (Corning, USA) was firstly covered with autoclaved agarose solution (1.5%, w/v) at 50 μL/well and then cooled to room temperature. Mixed HeLa and NIH3T3 cells (1:1) were seeded at a density of 2×10^3 cells per well and incubated for 4 days to grow into MCTS. The formation of MCTS was monitored using optical microscope (TE2000-S, Nikon, Japan).

Animal model: Female BALB/c nude mice (4-5 weeks, 16 g) purchased from Shanghai Laboratory Animal Center (SLAC, China) were maintained at 22 ± 2 °C with access to food and water ad libitum. All animal experiments were approved by the Animal Care and Use Committee of Zhejiang University in accordance with the guidelines for the care and use of laboratory animals. Single HeLa or HeLa/A549 co-bearing tumor xenograft model was established according to previous report with minor modifications [1]. Briefly, the suspensions of HeLa (1×10^7) or A549 (2×10^6) cells in 100 μl of phosphate buffer saline (PBS, 0.01 M, pH 7.4) were inoculated subcutaneously in the flank of nude mice. Tumor sizes were measured using a Vernier caliper, and tumor volumes were calculated as $V = a^2 \times b/2$ mm^3 (a: minor axis; b: major axis).

Preparation of hybrid nanoparticles: The synthesis of ACC-DOX was performed in accordance with previous report with minor modifications. [2] Briefly, $CaCl_2$ (200 mg) and DOX (0.4 mL, 10 mg/mL, aqueous solution) were dissolved in absolute ethanol (100 mL). The mixture were transferred into a glass bottle and covered by parafilm with several pores. The bottle was then left in a desiccator along with two glass bottles of $(NH_4)_2CO_3$ at 25 °C. After vapor diffusion reaction for 2-3 days, the products were centrifuged (Allegra 64R, Beckman Coulter, USA, 8,000 rpm, 10 min), rinsed several times and then re-dispersed in proper amount of absolute ethanol. Drug free ACC nanoparticles were prepared in the same way without DOX.

The ACC-DOX were then dispersed into ethanol containing PL (PL: ACC-DOX = 1, w/w) and 20% (w/w to PL) of DSPE-PEG and DSPE-PEG-FA (1:1, w/w). After stirring at 37 °C for 24 h, the mixture was ultrasonicated at 800 W at room temperature for 20 times (work 2 s and stand 3 s) by a Lab ultrasonic cell pulverizer (JY92-II, Ningbo Scientz Biotechnology Co., Ltd, China) and then centrifuged at 3,000 rpm for 10 min to remove unbounded free PL. The obtained supernatant was then injected (via an injection syringe) into water under moderate stirring at a volume ratio of 1:9 (ethanol:water). The obtained PL/ACC-DOX were further dialysis against distilled water (Milipore, USA) for 4 h (MWCO: 7 kDa, 2 L × 6) with gentle agitation to remove unloaded drugs, followed by storage at 4 °C until further use. Hybrid nanoparticles without FA modification were synthesized by replacing DSPE-PEG-FA with DSPE-PEG. Drug free PL/ACC nanoparticles were prepared in the same way using ACC nanoparticles. The nanoparticles adopted in the following experiments were all with FA modification unless otherwise stated. The nanoparticles with or without FA modification showed similar properties in size and zeta potential (data not shown).

***Synthesis of OA modified CCC-DOX (OA-CCC-DOX) nanoparticles*:** For the preparation of OA-CCC-DOX, $CaCl_2$ (555 mg) and DOX (4 mg) were charged into water (5 mL) at room temperature with gentle agitation to obtain a clear solution. $(NH_4)_2CO_3$ aqueous solution (1 M, 5 mL) was quickly added into the mixture under vigorously stirring for 30s.

Afterwards, OA (10 mg) contained cyclohexane (5 mL) was charged into the bottle and vigorously stirred for another 5 min. The resulted mixture was centrifuged at 3000 rpm for 10 min and the supernatant was collected. Excess ethanol (20 mL) was added and the mixture was further centrifuged at 3000 rpm for 10 min to precipitate the OA-CCC-DOX. The resulted OA-CCC-DOX were rinsed several times with absolute ethanol, re-dispersed in *n*-hexane and stored in 4°C until further use.

OA-CCC-DOX, PL and DSPE-PEG with the same w/w ratio as mentioned above were dispersed in mixed solution (2 mL, ethanol:*n*-hexane, 1:1, v/v). The mixture was ultrasonicated at 400 W at room temperature for 20 times (work 2 s and stand 3 s) by a Lab ultrasonic cell pulverizer (JY92-II, Ningbo Scientz Biotechnology Co., Ltd, China) to obtain homodispersed solution. The solution was then injected into water under moderate stirring. The reaction was proceeded for another 5 min and then ultrasonicated at 1000 W at room temperature for 40 times. Afterwards, the whole mixture was subjected to rotary evaporation under vacuum at 50 °C until a transparent solution was obtained. After being centrifuged at 3000 rpm for 10 min, supernatant was collected and further dialysis against distilled water (Milipore, USA) for 4 h (MWCO: 7 kDa, 2 L × 6) with gentle agitation to remove unloaded drugs.

Characterizations of nanoparticles: ACC-DOX in organic solvents were oven dried to obtain nanoparticle powder. Aqueous PL/ACC-DOX was centrifuged (20000 rpm, 10 min) to precipitate nanoparticles and then oven dried to obtain powder. The comparative FTIR (FT/IR-4100, JASCO, Japan) of different nanoparticles was investigated to study the chemical composition and interaction. The polymorph of ACC in different nanoparticles were recorded by XRD (Rotaflex RU-200, Rigaku, Japan). The XRD spectra of other components other than ACC-DOX in PL/ACC-DOX were used to normalize the XRD spectrum of PL/ACC-DOX.

The morphology and particle size of different nanoparticles were observed by transmission electron microscopy (TEM). Briefly, a drop of nanoparticle solution was deposited on a lacy carbon-coated cupper grid. The excess solution was removed by a piece of filter paper. The sample was air dried and observed under a TEM system (JEM-1200, JEOL, Japan) at an accelerating voltage of 80 kV. Moreover, the comparative particle size and zeta potential were further determined by Particle Sizer (Nano S90, Malvern Instruments Ltd., UK) and Zeta Analyzer (Litesizer 500, Anton Paar, Austria), respectively.

ACC-DOX and PL/ACC-DOX (without FA modifications) were prepared and then dispersed into water, their ultraviolet (UV) spectra between 400-750 nm were recorded by an ultraviolet-visible spectrophotometer (TU-1810, Purkinje, China). The UV spectrum of ACC-DOX in ethanol was employed as a control.

To eliminate the UV interference of DOX and FA, drug free ACC and PL/ACC (without FA modifications) with similar size were incubated with BSA aqueous solution (1 mg/mL) at the final ACC concentrations of 0.1, 0.2, 0.3, 0.4 and 0.5 mg/mL for 2 h at 37 °C. At the end of the incubation, samples were firstly centrifuged at 20000 rpm for 30 min and then filtrated through millipore syringe (0.22 μm). The variation of optical density (OD) at 278 nm was recorded and plotted against concentration. BSA aqueous solutions subjected to the same procedures were employed as blank control.

ACC-DOX and PL/ACC-DOX were incubated with 20% FBS at 37 °C for 2 h. Samples were measured at different time intervals and their changes in particle size were recorded.

***Drug release*:** The drug release profile of ACC-DOX and PL/ACC-DOX was investigated by dialysis method. Briefly, samples were placed into individual dialysis bag (MWCO: 7 KDa) and immersed in plastic tube containing 25 mL of phosphate buffer with pH of 7.4, 6.5 and 5.5, respectively. The plastic tubes were fixed in a thermostatic shaker (HZQ-C; Haerbin Dongming Medical Instrument Factory, China) at 37 °C with a stirring speed of 100 rpm. At predetermined time intervals, buffer solution within the tubes was removed for analysis and replaced with equal volume of fresh medium. The drug concentration was

determined by fluorescence spectrophotometer (F-2500, Hitachi Co., Japan) with excitation wavelength, emission wavelength and slit openings set at 505, 605, and 5 nm, respectively. [3]

In vitro targeting assay: To investigate the *in vitro* targeting potential of DSPE-PEG-FA modified hybrid nanoparticles, Hela as a FR overexpressed cell line and A549 as a FR deficient cell line were employed in our study. In order to exclude the cytotoxicity influence of DOX which might reduce the cell viability. C6 as a model fluorescent molecule was entrapped in the drug free PL/ACC nanoparticles during the preparation procedure. HeLa and A549 cells were seeded onto 35-mm glass-bottom culture dishes (Corning, USA) at a density of 1×10^5 cells per well and cultured overnight for 50-60 % confluence. To investigate whether nanoparticles were taken up through folate receptor (FR) mediated endocytosis, cells were incubated with excess amount of free FA for 1 hour prior to nanoparticles addition. The media were replaced by fresh serum-free medium containing PL/ACC. After 2, 4, and 6 h of incubation, the culture media were removed, and the cells were rinsed with PBS thrice. Subsequently, the cells were fixed with 4 % paraformaldehyde (15 min), followed by staining with Hoechst 33342 (10 μg/mL) for 15 min. Samples were observed and imaged under confocal laser scanning microscopy (CLSM, BX61W1-FV1000, Olympus, Japan). Quantitative uptake of nanoparticles was further investigated by flow cytometry (FCM, FC500MCL, Beckman Coulter, USA).

In vitro drug release: HeLa cells were seeded onto 35-mm glass-bottom and cultured as described above. After that, the primary culture media were removed and replaced with equal volume of serum-free medium containing free DOX, PL/ACC-DOX or PL/CCC-DOX (final Cur concentration: 20 μg/mL) for . At predetermined co-incubation time, cells were washed several times by PBS, fixed with paraformaldehyde and stained with Hoechst 33342. Samples were subjected to CLSM observation.

Cells cultured under the same condition as described above were adopted. Cells were firstly incubated with Hank's balanced salt solution (HBSS) containing nanoparticles (1 mg/mL) at 37 °C for 2 h. At the end of incubation, Fluo-4 AM (5 μM) was added to incubate with cells for 30 min. Afterwards, cells were rinsed with fresh HBSS and then subjected to CLSM observation. Live cell imaging was recorded every 10 s for 10 min to obtain the dynamic distribution behavior of calcium within the cells.

Cells cultured under the same condition as described above were adopted. To observe the intracellular trafficking of PL/ACC-DOX, cells were firstly incubated with HBSS containing PL/ACC-DOX at 37 °C for 4 h. At the end of incubation, Fluo-4 AM (5 μM) and Lyso tracker Blue (50 nM) were added to incubate with cells for 30 min and 15 min, respectively. Afterwards, cells were rinsed with fresh HBSS and then subjected to CLSM (Nikon A1R, Nikon, Japan) observation.

Drug penetration study: The MCTS was incubated with the free DOX, PL/ACC-DOX or PL/CCC-DOX at the DOX concentration of 1 μg/mL for 24 h, respectively. Then, the tumor spheroids were washed thrice with ice-cold PBS, fixed with paraformaldehyde for 30 min, and placed in cavity microscope slides. The images of the tumor spheroids were acquired by tomoscan using Z-stack imaging with 5 μm intervals from the top of the spheroid to the middle by CLSM.

When the tumor volume reached 200 mm^3, the HeLa tumor-bearing nude mice were intravenously administrated by PL/ACC-DOX or PL/CCC-DOX at a dose of 2 mg DOX/kg, respectively. At 48 h post-injection, tumors were collected and washed by PBS, followed by cryotomy. The frozen tumor sections were stained by DAPI (Solarbio Life Science, China) according to the manufacturer's instructions, followed by observation under CLSM. [4]

In vitro cytotoxicity: For the cell viability measurements, 200 μL of HeLa cells (1×10^4 cells/mL) in DMEM suspension was seeded in 96-well plates (Corning, USA) and allowed to culture overnight. The mediums were discarded and all wells were washed twice with fresh PBS. Subsequently, 200 μL of serum-free medium was added to each well, in which DOX or

nanoparticles was diluted to achieve the designated concentrations. After proper incubation, the cell viability was assessed with standard MTT assay. [5] Briefly, the medium was replaced with an equal volume of fresh medium containing 5 mg/mL MTT and incubated for 4 h at 37 °C. Then MTT was removed, and cells were lysed with dimethyl sulfoxide (DMSO) with stirring for 15 min on a microtiter plate shaker. The cell viability was estimated according to the absorption values determined by a microplate reader (Bio-Rad, model 680, USA) at the wave length of 570 nm. MCTS with diameters of 300-400 μm were divided into four groups (n = 3). The selected spheroids were treated with fresh medium containing free DOX, PL/ACC-DOX or PL/CCC-DOX (DOX concentration 1 μg/mL). Untreated MCTS was employed as control. The spheroids were allowed to continue to incubate at 37 °C for 5 days. The diameter of the spheroids was recorded every day using an optical microscope.

In vivo tumor targeting assay: For *in vivo* imaging analysis, near-infrared (NIR) probe DiR was loaded into the lipid matrix of PL/ACC-DOX during the preparation procedure. Subsequently, DiR-loaded PL/ACC-DOX were intravenously injected into the tumor-bearing nude mice (tumor volume 200 mm^3) at a dose of 50 μg DiR/kg to investigate their biodistribution and tumor-targeting efficacy (n = 3). At 6, 12, 24 and 36 h post-injection, the NIR fluorescent images were captured at an excitation wavelength of 740 nm and an emission wavelength from 740-950 nm using an *in vivo* imaging system (Maestro *In-vivo* Imaging System, USA). After living imaging, mice were sacrificed, the main organs and tumor tissues were excised for *ex vivo* imaging using the same imaging system. In addition, tumors were collected, followed by cryotomy and then subjected CLSM observation.

In vivo antitumor assay: When tumor volume reached around 50 mm^3, the *in vivo* antitumor efficacy of PL/ACC-DOX was evaluated on HeLa tumor xenograft models. Mice were randomly divided into 4 groups (n = 6), and intravenously injected by the saline, free DOX, PL/ACC-DOX or PL/CCC-DOX (DOX concentration 2 mg/kg). The initial day of administration was defined as Day 0, and administration was then repeated once every 2 days over a 14-day therapeutic period. The tumor volume and body weights of mice were measured before the administration. The rate of survival was calculated based on Kaplan–Meier plot for up to 60 days. At Day 14, mice in each group were randomly selected and euthanized. The main organs (heart, liver, spleen, lung and kidney) and tumor were collected, weighed, washed with saline thrice and fixed in 10% formalin. Formalin-fixed main organs and tumors were embedded in paraffin blocks to prepare sections and then subjected to hematoxylin-eosin (HE), TUNEL or Ki67 staining, respectively. Tissue images were captured at 200× magnification with the optical microscope.

Statistical analysis: Quantitative data were presented as mean ± standard deviation (S.D.) from triplicate experiments performed in a parallel manner unless otherwise noted. Statistical significance was tested by two-tailed Student's t-test or one-way ANOVA $*P < 0.05$ or $**P < 0.01$was considered statistically significant.

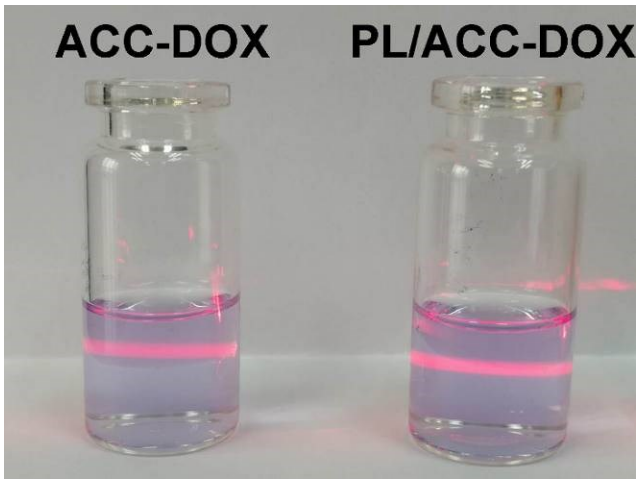

Fig. S1. The colloidal solution and Tyndall light scattering images of ACC-DOX and PL/ACC-DOX.

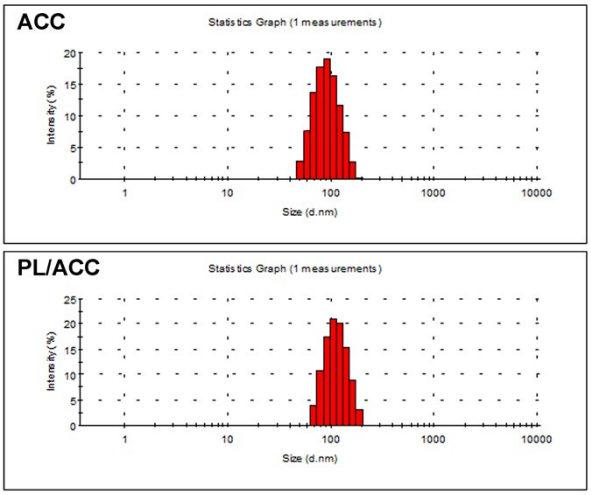

Fig. S2. Size distribution of ACC and PL/ACC determined by dynamic light scattering method.

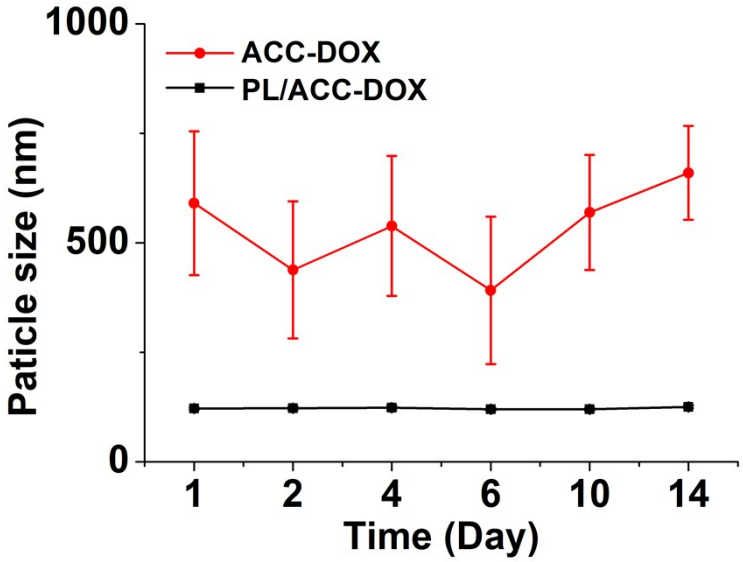

Fig. S3. Stability test of ACC-DOX and PL/ACC-DOX under physiological condition (PBS, pH 7.4) for two weeks. Results were expressed as mean ± S.D. (n = 3).

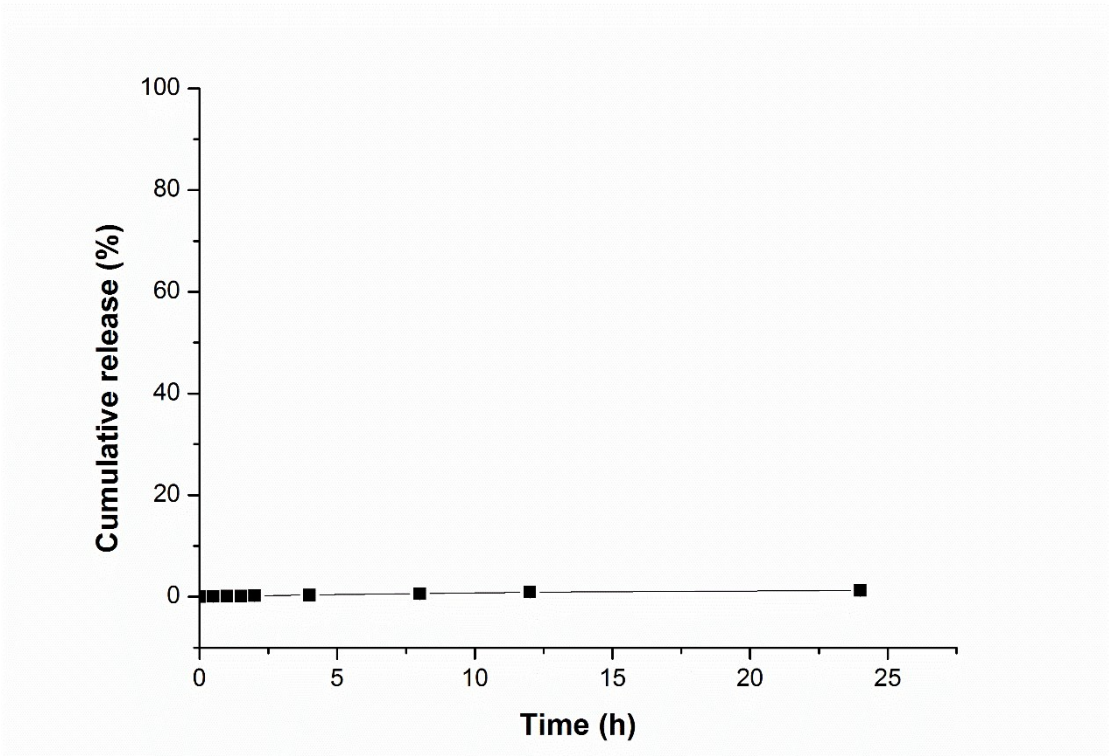

Fig. S4. *In vitro* drug release of DOX from ACC-DOX in ethanol for 24 h. Results were expressed as mean ± S.D. (n = 3).

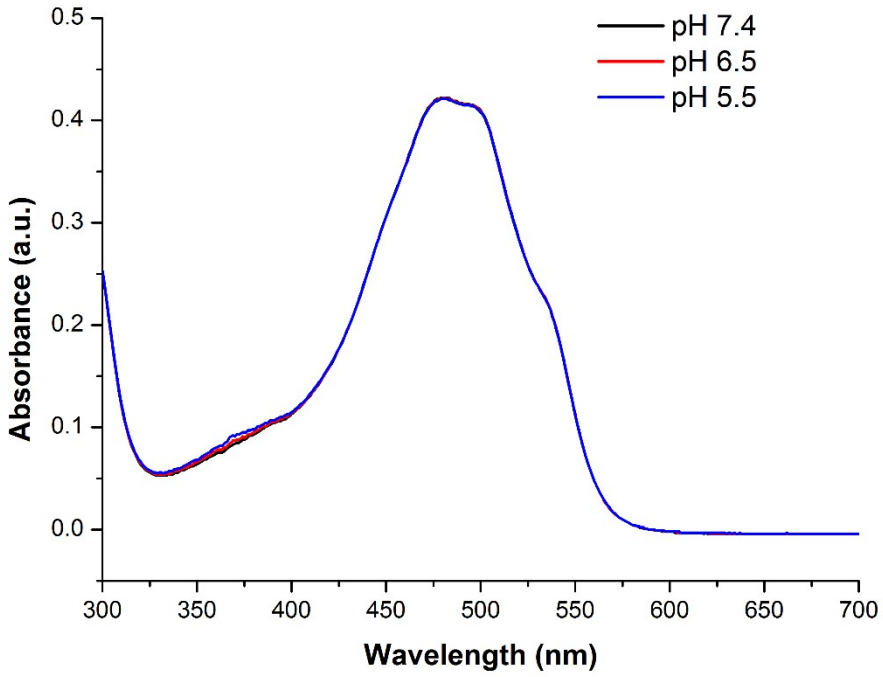

Fig. S5. UV spectra of the released DOX from ACC-DOX in various pH conditions (7.4, 6.5, and 5.5). When the ACC-DOX were charged into in aqueous solutions, the resulted supernatant of solutions (8000 rpm, 5 min) showed the featured absorption peak of DOX at 480 nm.

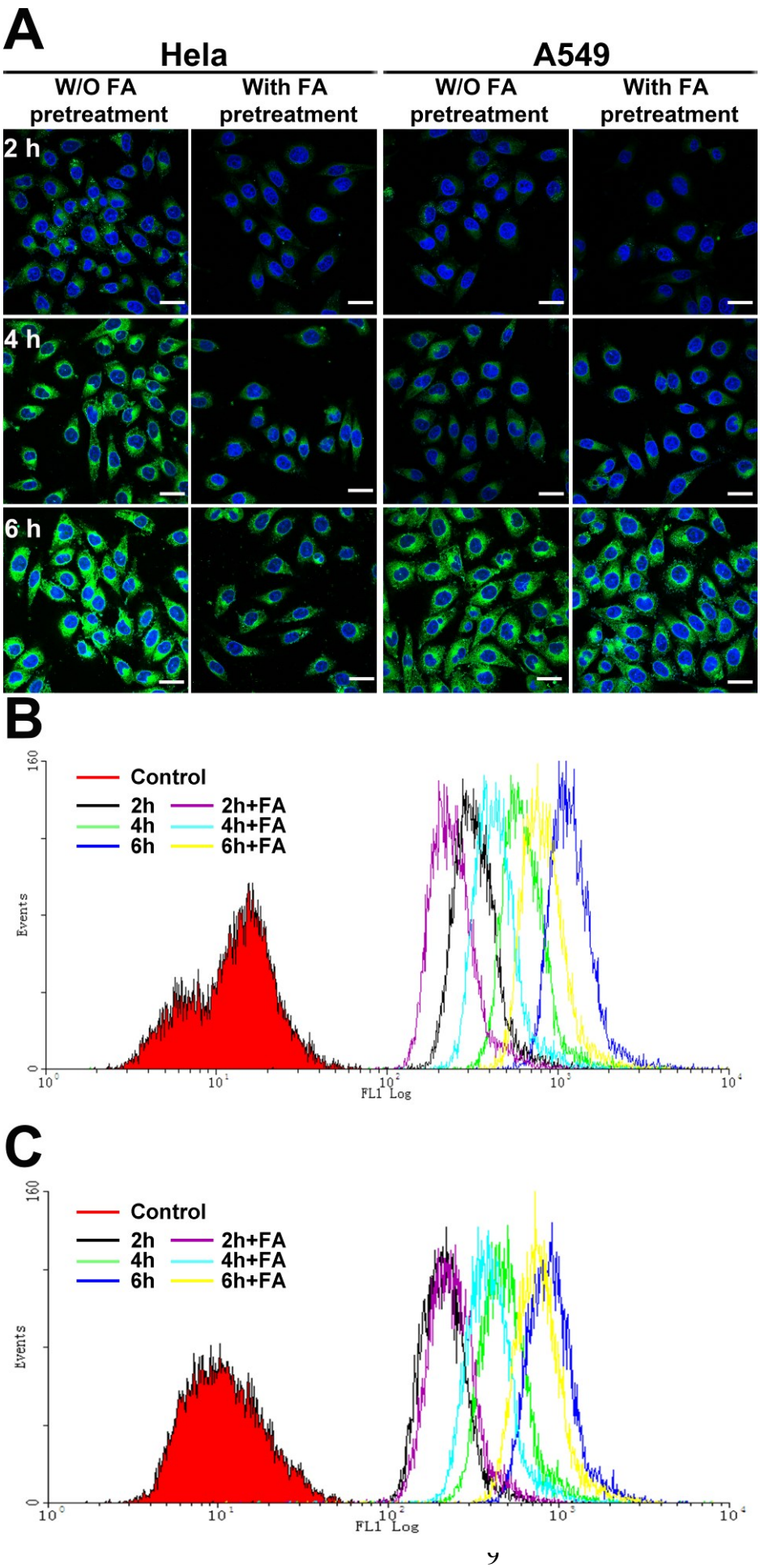
A
Hela
A549
W/O FA pretreatment
With FA pretreatment
W/O FA pretreatment
With FA pretreatment
2 h
4 h
6 h
B
Control
2h
2h+FA
4h
4h+FA
6h
6h+FA
Events
FL1 Log
C
Control
2h
2h+FA
4h
4h+FA
6h
6h+FA
Events
FL1 Log

Fig. S6. (A) *In vitro* cellular uptake of C6 loaded PL/ACC nanoparticles with and without pretreatment with excess amount of free FA in HeLa and A549 cells as a function of incubation time (2, 4 and 6 h). For each panel, blue: Hoechst 33342 stained nuclei; Green: C6 indicated nanoparticles. Scale bar: 20 μm. Flow cytometric curves representing the fluorescence signal of C6 loaded PL/ACC with/without pretreatment with excess amount of free FA for different incubation period (2, 4 and 6 h) in HeLa (B) and A549 (C) cells. Each analysis was generated by counting 10^4 cells.

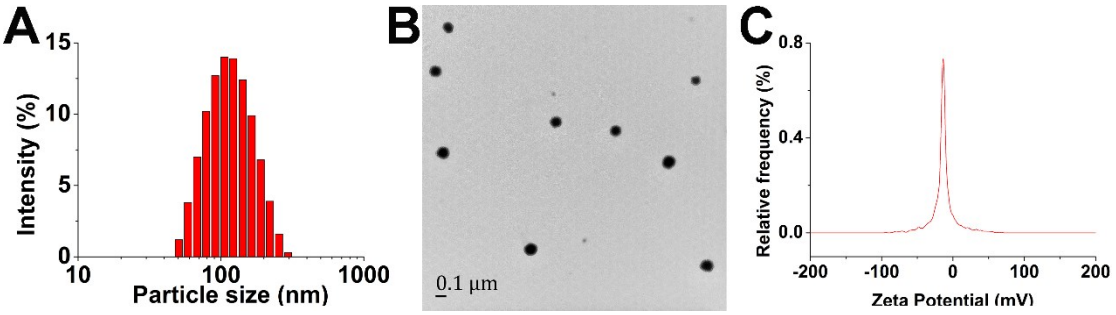

Fig. S7. Representative size distribution (A), TEM (B) image and zeta potential (C) of PL/CCC-DOX. Scale bar: 100 nm.

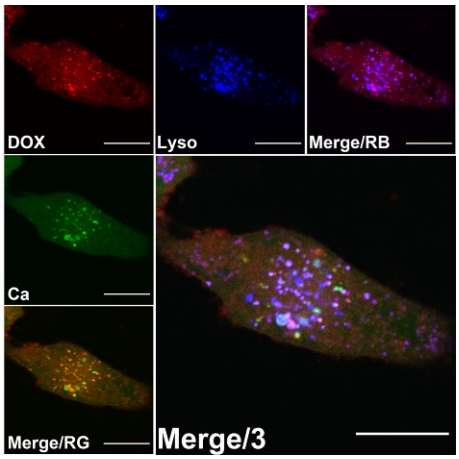

Fig. S8. Intracellular trafficking of PL/ACC-DOX nanoparticles in HeLa cells at 4 h post incubation. For each panel, Ca: Fluo-4 AM indicated Ca^{2+} (green); Lyso: Lyso-tracker Blue stained endo-lysosome (blue); DOX: DOX (red); Merge/RB: merge of DOX and endo-lysosome (purple); Merge/RG: merge of DOX and Ca^{2+} (yellow); Merge/3: merge of all three colors. Scale bars: 20 μm.

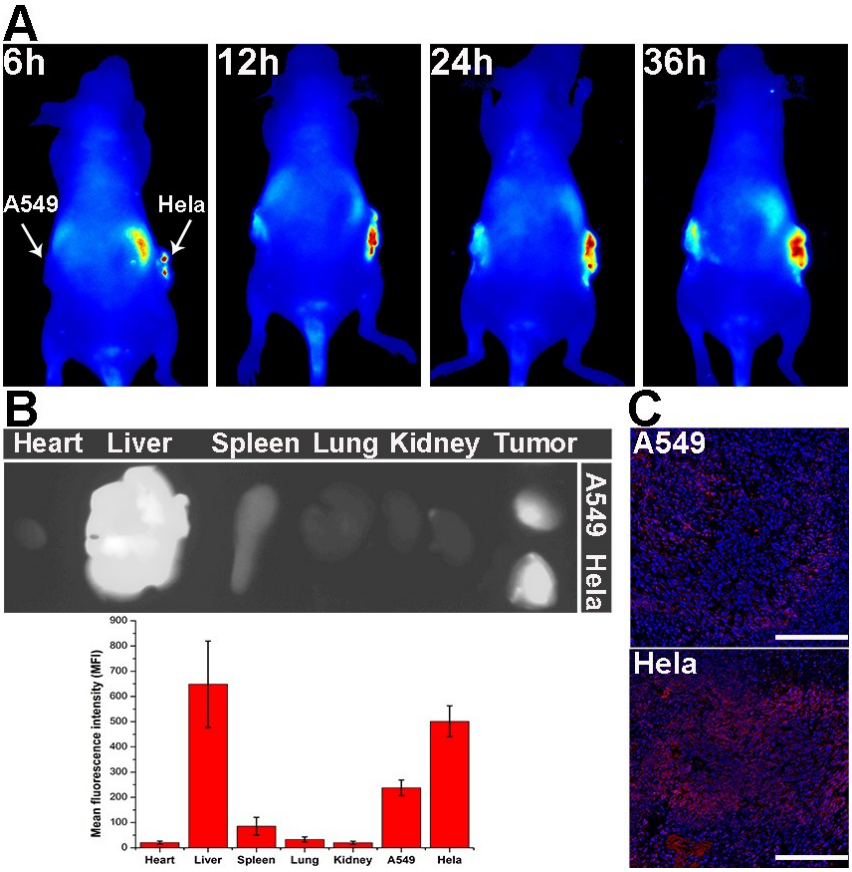

Fig. S9. *In vivo* tumor targeting assay of DiR loaded PL/ACC-DOX nanoparticles. (A) Real time *in vivo* distribution of nanoparticles in oxgraft model co-bearing HeLa and A549 tumors. (B) Representative *ex vivo* NIR fluorescence images and semi-quantitative analysis of dissected main organs and tumors at 36 h post-injection. Semi-quantitative was calculated as photo flux per mm^2 of tissues. Results were expressed as mean ± S.D. (n = 3). (C) CLSM imaging of slides obtained from frozen HeLa and A549 tumors. The cell nuclei were stained with DAPI (blue), DOX signal were shown as red. Scale bar: 200 μm.

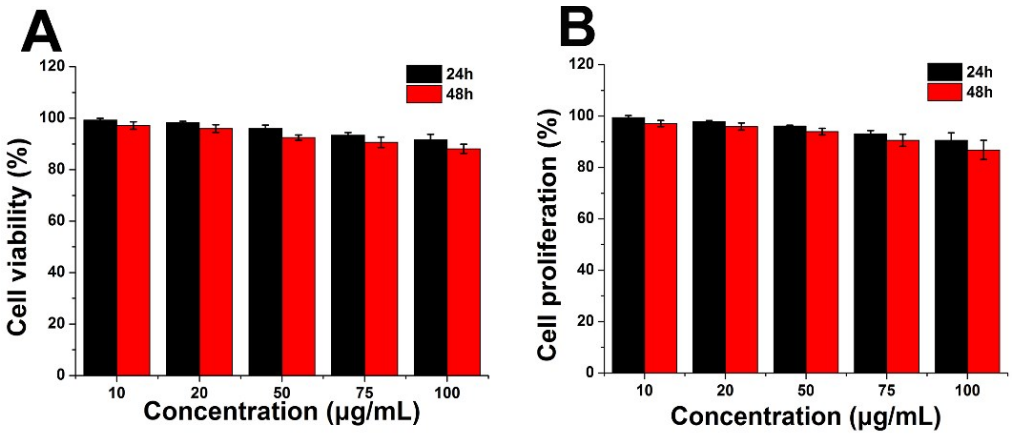

Fig. S10. Cell viabilities of HeLa cells incubated with drug free PL/ACC (A) and PL/CCC (B) at different nanoparticle concentrations (10-100 μg/mL) for 24 and 48 h, respectively. Results were expressed as mean ± S.D. (n = 3).

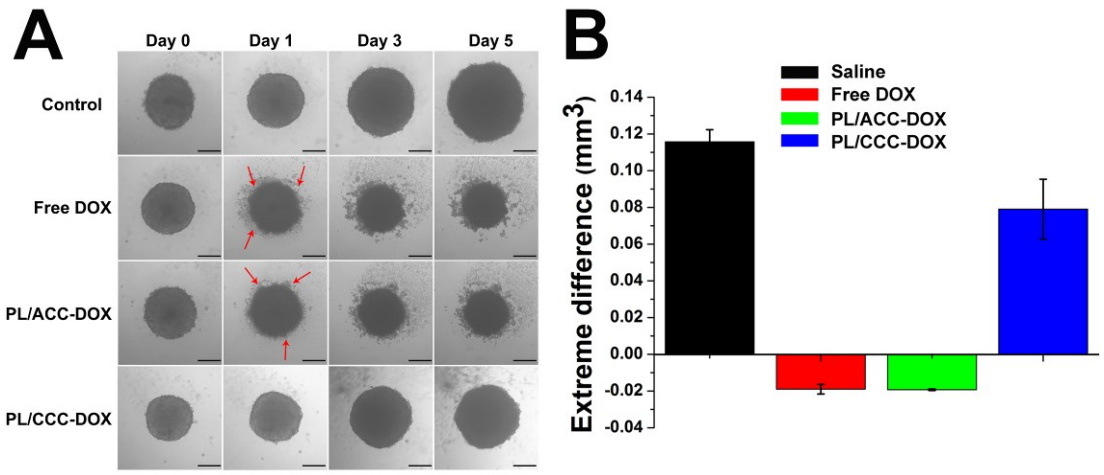

Fig. S11. (A) Extreme difference of MCTS (between Day 0 and Day 5) treated with with saline, free DOX, PL/ACC-DOX or PL/CCC-DOX nanoparticles (DOX concentration: 1 μg/mL). (B) Optical images of MCTS after treated with different formulations. The arrows indicate the cell fragments shedding from the surface of the tumor spheroids. Scale bars: 200 μm. Results were expressed as mean ± S.D. (n = 3).

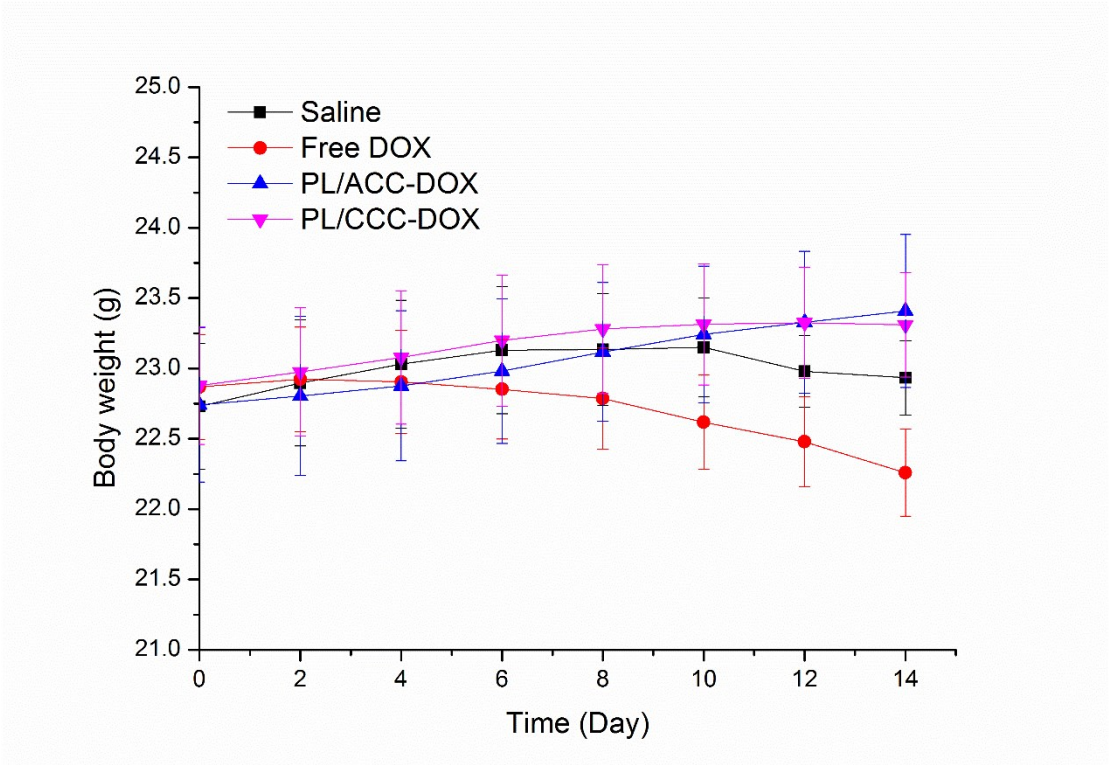

Fig. S12. The body weight analysis of HeLa tumor-bearing BALB/c nude mice after intravenous administration of saline, free DOX, PL/ACC-DOX or PL/CCC-DOX, respectively. The measurement of body weight was repeated every 2 days for two weeks. Dose: 2 mg DOX/kg. Results were expressed as mean ± S.D. (n = 6).

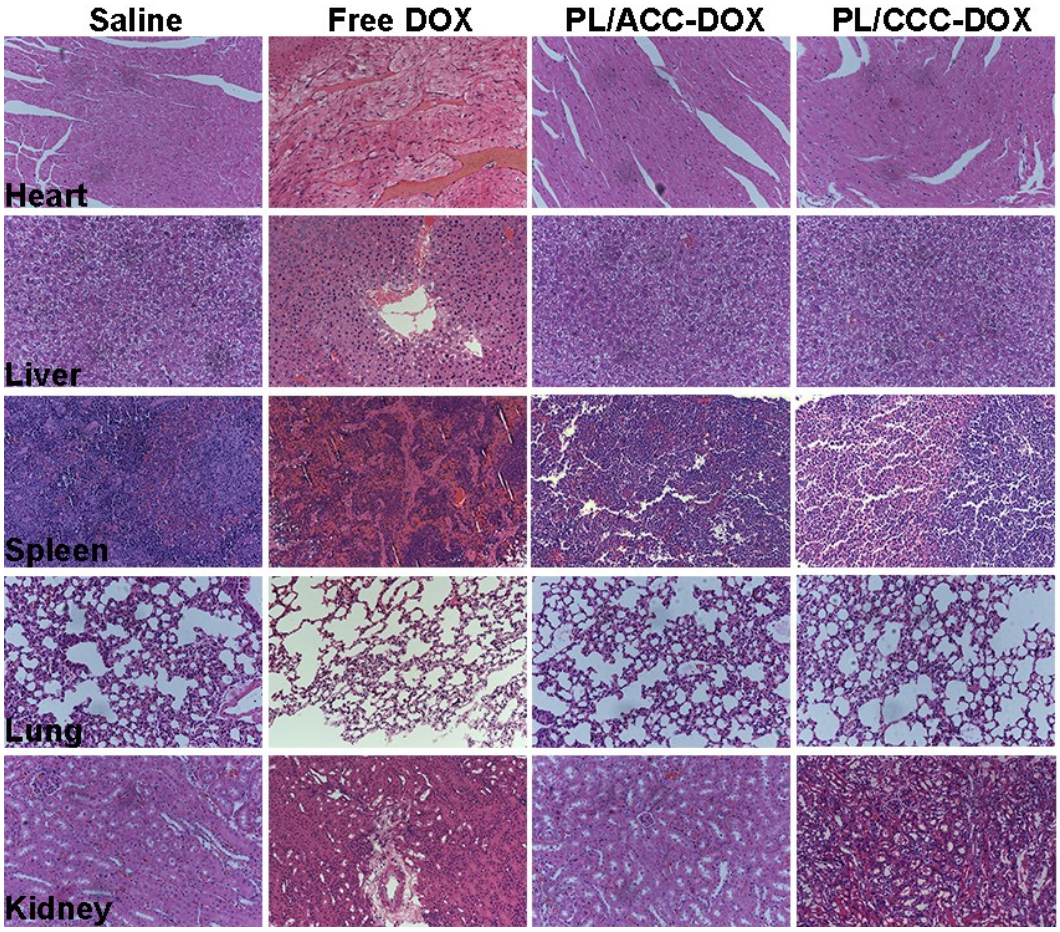

Fig. S13. Representative images (200×) of main organs (Heart, Liver, Spleen, Lung and Kidney) separated from mice after HE staining. It can observed that DOX showed evident pathological changes, especially cardiology, on organs.

Movie S1.avi

Movie S1. Time-dependent variation of intracellular Ca^{2+} concentration (monitored by Fluo-4 AM for 10 min) in HeLa cells treated with PL/ACC-DOX.

Movie S2.avi

Movie S2. Time-dependent variation of intracellular Ca^{2+} concentration (monitored by Fluo-4 AM for 10 min) in HeLa cells treated with PL/CCC-DOX.

[1] C. Wang, X. Bao, X. Ding, Y. Ding, S. Abbad, Y. Wang, M. Li, Y. Su, W. Wang, J. Zhou, Polymer Chemistry 2015, 6, 780.
[2] Y. Zhao, Z. Luo, M. Li, Q. Qu, X. Ma, S. H. Yu, Y. Zhao, Angew Chem Int Ed Engl 2015, 54, 919.
[3] H. Yuan, C. Y. Chen, G. H. Chai, Y. Z. Du, F. Q. Hu, Molecular Pharmaceutics 2013, 10, 1865.
[4] C. Ju, R. Mo, J. Xue, L. Zhang, Z. Zhao, L. Xue, Q. Ping, C. Zhang, Angewandte Chemie 2014, 53, 6253.
[5] D. Han, W. Fang, R. Zhang, J. Wei, N. D. Kodithuwakku, L. sha, W. Ma, L. liu, F. Li, Y. Li, Brain, Behavior, and Immunity 2016, 51, 56.